HHS Public Access

Author manuscript

Sci Immunol. Author manuscript; available in PMC 2023 February 25.

Published in final edited form as:

Sci Immunol. 2021 October 29; 6(64): eabj1181. doi:10.1126/sciimmunol.abj1181.

Salmonella Typhi Vi capsule prime-boost vaccination induces convergent and functional antibody responses

Lindsay C. Dahora[1,2,*,†], **Marije K. Verheul**[3,†], **Katherine L. Williams**[4], **Celina Jin**[3], **Lisa Stockdale**[3], **Guy Cavet**[4], **Eldar Giladi**[4], **Jennifer Hill**[3], **Dongkyoon Kim**[4], **Yvonne Leung**[4], **Benjamin G. Bobay**[5,6,7], **Leonard D. Spicer**[5,6,7], **Sheetal Sawant**[1,8], **Sjoerd Rijpkema**[9], **S. Moses Dennison**[1,8], **S. Munir Alam**[10,11,12], **Andrew J. Pollard**[3,‡], **Georgia D. Tomaras**[1,2,8,13,*,‡]

[1]Center for Human Systems Immunology, Duke University, Durham, NC, USA.

[2]Department of Immunology, Duke University, Durham, NC, USA.

[3]Oxford Vaccine Group, Department of Pediatrics, University of Oxford and NIHR Oxford Biomedical Research Center, Oxford, UK.

[4]Atreca Inc., San Carlos, CA, USA.

[5]Department of Biochemistry, Duke University, Durham, NC, USA.

[6]Department of Radiology, Duke University, Durham, NC, USA.

[7]Duke University NMR Center, Duke University Medical Center, Durham, NC, USA.

[8]Department of Surgery, Duke University, Durham, NC, USA.

[9]Division of Bacteriology, National Institute of Biological Standards and Control, Potters Bar, UK.

[10]Department of Medicine, Duke University, Durham, NC, USA.

[11]Department of Pathology, Duke University, Durham, NC, USA.

[12]Duke Human Vaccine Institute, Duke University, Durham, NC, USA.

[13]Department of Molecular Genetics and Microbiology, Duke University, Durham, NC, USA.

Abstract

*Corresponding author. lcd26@duke.edu (L.C.D.); gdt@duke.edu (G.D.T.).
†These authors contributed equally to this work.
‡These authors contributed equally to this work.

Author contributions: L.C.D., M.K.V., K.L.W., C.J., G.C., D.K., Y.L., J.H., A.J.P., and G.D.T. designed the study. Laboratory experiments were carried out by L.C.D., M.K.V., K.L.W., and Y.L. Data were analyzed and interpreted by L.C.D., M.K.V., K.L.W., L.S., G.C., E.G., D.K., Y.L., J.H., B.G.B., L.D.S., A.J.P., and G.D.T. L.C.D. and M.K.V. wrote the first draft. A.J.P. and G.D.T. edited, and all authors reviewed and approved the final version of the manuscript.

Competing interests: A.J.P. is chair of UK Department of Health and Social Care's (DHSC) Joint Committee on Vaccination and Immunisation (JCVI) and is a member of the WHO's SAGE. A.J.P. is an NIHR Senior Investigator. The views expressed in this article do not necessarily represent the views of DHSC, JCVI, NIHR, or WHO. A.J.P. is chief investigator on clinical trials of Oxford University's COVID19 vaccine, funded by NIHR. Oxford University has entered a joint COVID19 vaccine development partnership with AstraZeneca.

Vaccine development to prevent *Salmonella* Typhi infections has accelerated over the past decade, resulting in licensure of new vaccines, which use the Vi polysaccharide (Vi PS) of the bacterium conjugated to an unrelated carrier protein as the active component. Antibodies elicited by these vaccines are important for mediating protection against typhoid fever. However, the characteristics of protective and functional Vi antibodies are unknown. In this study, we investigated the human antibody repertoire, avidity maturation, epitope specificity, and function after immunization with a single dose of Vi-tetanus toxoid conjugate vaccine (Vi-TT) and after a booster with plain Vi PS (Vi-PS). The Vi-TT prime induced an IgG1-dominant response, whereas the Vi-TT prime followed by the Vi-PS boost induced IgG1 and IgG2 antibody production. B cells from recipients who received both prime and boost showed evidence of convergence, with shared V gene usage and CDR3 characteristics. The detected Vi antibodies showed heterogeneous avidity ranging from 10 μM to 500 pM, with no evidence of affinity maturation after the boost. Vi-specific antibodies mediated Fc effector functions, which correlated with antibody dissociation kinetics but not with association kinetics. We identified antibodies induced by prime and boost vaccines that recognized subdominant epitopes, indicated by binding to the de–*O*-acetylated Vi backbone. These antibodies also mediated Fc-dependent functions, such as complement deposition and monocyte phagocytosis. Defining strategies on how to broaden epitope targeting for *S.* Typhi Vi and enriching for antibody Fc functions that protect against typhoid fever will advance the design of high-efficacy Vi vaccines for protection across diverse populations.

INTRODUCTION

Vaccines are designed to induce a protective immune response against pathogens through the induction of functional antibodies (1). Correlates or surrogates of protection are often based on antibody levels (e.g., *Haemophilus influenzae* type b, hepatitis B vaccines) (2), although in many cases, protective antibody thresholds are difficult to reproduce. Few vaccines have mechanistic correlates, such as those measured in a serum bactericidal assay (e.g., meningococcal vaccines) or opsonophagocytosis assay (e.g., pneumococcal vaccines) (1, 3). Hence, increased attention is needed on not only the quantity but also the quality of the antibody response. Where quantitative antibody features fail, qualitative features such as specificity and affinity play a crucial role in protection against various pathogens including HIV-1, malaria, Zika, and others (4–7). In addition, antibody repertoire sequencing and single-cell B cell receptor (BCR) sequencing have provided insight into antibody development and selection upon immunization. Studying antibody responses after immunization and infection is therefore important to determine the antibody specificities that impart protection or control and, ultimately, for the development and optimization of vaccines.

One of the more recently developed vaccines for the prevention of typhoid fever is a Vi typhoid conjugate vaccine (Vi-TCV), in which Vi capsular polysaccharide antigen (Vi PS) is conjugated to tetanus toxoid (Vi-TT). Vi-TT induces immune responses that target Vi PS of *Salmonella enterica* subspecies *enterica* serovar Typhi (*S.* Typhi) (8). This bacterial pathogen infects 10 million to 13 million people annually (9) and is evolving to display extensive antibiotic resistance (10, 11). Immunogenicity of Vi-TT was established in a non-endemic population using a controlled human infection model (CHIM), where the efficacy was found

to be comparable to the licensed plain Vi PS vaccine (Vi-PS) (12). After this, a Vi-TT efficacy of 82% was observed in a randomized, controlled trial in typhoid-endemic Nepal (13). Both studies reported an increase in anti-Vi immunoglobulin G (IgG) antibodies after immunization; however, estimates on thresholds of Vi IgG required for protection have been difficult to reproduce for decades (14, 15). Recently, we reported that Vi PS–specific IgG1 avidity and IgA magnitude and fold change were associated with protection in a CHIM study (16, 17). Although Vi vaccination is widely used to protect against typhoid fever, data on repertoire and functionality of antibodies induced after Vi immunization are currently limited. Understanding how to broaden the specificities and functional antibody repertoire will inform further immunogen design to protect against typhoid fever.

The Vi PS antigen constitutes one of the major virulence factors of *S.* Typhi as it shields the bacterial cell from the innate immune system upon entry through the gastrointestinal tract (18, 19). The Vi PS antigen is a linear homopolymer of α−1→4-galacturonic acid with variable *O*-acetylation (60 to 90% in naturally occurring *S.* Typhi) at the C3 position and a fixed *N*-acetyl at the C2 position (20, 21). Immunogenicity and antigenicity data have shown that the immunodominant epitope of Vi PS is the C3 *O*-acetyl group. This has been explained through molecular dynamics simulations showing that the *O*-acetyl is solvent-exposed and bulky, thus burying the polysaccharide backbone and occluding alternative epitopes (22). However, partial de–*O*-acetylation (~45% *O*-acetylated Vi) has been shown to increase immunogenicity of Vi PS antigen (20), possibly owing to increased flexibility in the polysaccharide backbone (22). These studies have resulted in a World Health Organization standard for formulation of Vi vaccines to include Vi PS antigen with at least 52% [Vi (2 mmol/g)] of monomers *O*-acetylated at C3 (23). Despite the immunodominance of the C3 *O*-acetyl group, studies have shown that the vaccine still induces rabbit and human sera that exhibit binding to de–*O*-acetylated Vi PS antigen, albeit at very low levels (20, 22). The binding to de–*O*-acetylated Vi PS antigen after vaccination indicates that vaccine-elicited antibodies also target non–*O*-acetyl alternative epitopes, likely the C2 *N*-acetyl and/or the C5 carboxyl, which has been shown by one mouse monoclonal antibody (mAb) (24, 25). These epitopes may be subdominant but still solvent-exposed (SEE) or buried beneath the bulky *O*-acetyl group and occluded (SEO). To date, the repertoire of antibodies generated toward Vi PS antigen and their functional relevance in humans have not been explored.

Here, we evaluate the B cell repertoire of antibodies elicited by Vi vaccination in humans, determine which epitope specificities are present, investigate their avidity for Vi PS antigen, and establish their ability to mediate Fc-dependent effector functions. We show evidence of a heterogeneous antibody response with regard to antibody repertoire, IgG subclass distribution, and affinity maturation after both prime (Vi-TT) and boost (Vi-PS). We identified Vi PS antigen–specific antibodies using selection strategies based on sequence convergence and the expansion and persistence of B cell lineages. At least four subdominant, alternative epitopes targeted by vaccine-elicited antibodies were identified including two epitopes that are shielded by the *O*-acetyl group and two epitopes that are exposed regardless of the presence of *O*-acetyl. Antibodies targeting the exposed epitopes can mediate antibody-dependent monocyte phagocytosis (ADMP) and antibody-dependent complement deposition (ADCD) with a magnitude that significantly correlates with antibody-antigen off-rate kinetics.

RESULTS

Vi-PS and Vi-TT immunizations induce a diverse antibody response with differences in variable heavy chain and subclass usage

A total of 12 participants were recruited to be immunized with Vi-TT, followed by a Vi-PS boost, and 10 participants completed the study. A subset of eight participants was selected on the basis of peripheral blood mononuclear cell (PBMC) availability. Paired data after both immunizations were available for only three of these eight participants, whereas for the remaining five participants, data were available only after the Vi-PS boost. IgG-positive plasmablasts collected from participants 7 days after prime with Vi-TT ($n = 3$) and 7 days after boost with Vi-PS ($n = 8$) were used for single-cell BCR sequencing (fig. S1). Humoral responses measured after Vi-PS boost represent both memory B cell responses induced by the Vi-TT prime in addition to naïve B cell responses induced by the Vi-PS boost. Because Ig subclasses are major determinants of antibody functionality, we investigated the subclass distribution within identified BCRs. After Vi-TT primary immunization, the predominant subclass was IgG1 (81.9 to 86.5%), with a small percentage of IgG2 (10.2 to 15.9%). In the paired samples after the Vi-PS boost, IgG1 (50.1 to 65.6%) remained the most prevalent, but increased percentages of IgG2 antibodies (28.1 to 46.5%) were observed. IgG2 sequences were also prevalent in the additional nonpaired Vi-PS samples (38.8 to 80.0%), compared with IgG1 (17.2 to 49.3%). IgG3 and IgG4 formed a very small proportion of the total BCRs identified (up to 13.2%; Fig. 1A).

To further characterize the observed heavy-chain sequences, additional features corresponding to functionally mature antibodies were investigated. The complementarity-determining region 3 (CDR3) lengths after both Vi-TT prime and Vi-PS boost immunizations showed the expected Gaussian distribution, with little difference (Fig. 1B). The heavy-chain CDR3 length distributions for individual vaccinees included sharp peaks at particular lengths, suggesting that there were marked expansions of specific B cell clones after immunization (Fig. 1, C to E, and fig. S2). All six CDR3 length distributions deviate from a normal distribution (Shapiro-Wilk normality test, $P < 0.001$ for each). In addition, some of the heavy-chain V genes were overrepresented after either the Vi-TT prime or the Vi-PS boost immunization (Fig. 1F and fig. S3), suggesting that the prime and booster shots elicit antibody responses with different characteristics. These differences (Fig. 1) could be due, in part, to recall of memory cells after the boost. Thus, the Vi-TT primary immunization largely induced an IgG1 immune response, whereas the Vi-PS boost induced a response with both IgG1 and IgG2. In addition, the sequence analysis indicated that clonal expansion occurred after both immunizations.

Selection based on convergence, expansion, and persistence results in successful identification of Vi-specific antibodies

To identify Vi PS antigen–specific antibodies within the studied repertoires, antibodies were selected for expression as recombinant protein based on three approaches. Antibodies from individual participants were grouped into families based on the same predicted V_H/J_H and V_L/J_L germline gene usage and with V_H and V_L CDR3 sequences of equal lengths. The first approach was to favor the largest expanded families. Because expansion of antigen-

specific plasmablasts is expected 7 days after immunization, larger families are more likely to represent the humoral response to the vaccine. Most families contained only one or two sequences, with only a small proportion showing greater expansion (Fig. 2A and fig. S4). Only families expanded after the Vi-PS booster immunization were selected in this approach. The second approach was to identify antibody family persistence by selecting families that were observed after the prime immunization and also present and expanded in the same participant after the Vi-PS boost (Fig. 2B). The persistent observation of a family after both immunizations is consistent with activation by the Vi component of both vaccines instead of the TT component of the Vi-TT prime. In the third approach, antibodies were prioritized on the basis of convergence across participants (Fig. 2C). A total of 96 families were selected on the basis of a combination of expansion, persistence, and convergence (Fig. 2D), and one representative of each family was picked to generate 96 mAbs.

Of 96 generated mAbs, 53 (55%) were positive for Vi PS antigen binding by biolayer interferometry (BLI) ranging from low-level binding at the 0.08-nm positivity cutoff to high binding with a maximum of 13.22 nm (Fig. 2E). For one of eight participants, none of the selected antibodies bound to Vi PS antigen. Antibodies selected for convergence had the highest rate of Vi PS antigen binding (63%), followed by 50% for persistence and 47% for expansion (Fig. 2F). This is consistent with the induction of convergent antibody responses (similar antibodies in different participants) by Vi vaccines. Although selection of the mAbs was carried out independently of the CD62L status of the plasmablast that was used for BCR sequencing, CD62L-positive plasmablasts were associated with a higher frequency of Vi PS antigen binding ($P < 0.008$; Fig. 2G): 70% of the selected CD62L-positive plasmablasts were positive for Vi PS antigen binding, whereas only 40% of the CD62L-negative plasmablasts were positive for Vi PS antigen binding. Of the 96 mAbs, only 2 were found to bind TT (fig. S5). Combined, these data indicate that the selection strategy performed here was successful and could potentially be improved by incorporating CD62L status. To investigate maturation of the antibody response to Vi, we examined the number of somatic hypermutations in the variable regions of the antibody heavy and light chains after prime and boost. The range of the mutation rate for post-prime mAbs was between 11 and 34 mutations and 2 and 47 mutations after boost (fig. S6). This level of somatic hypermutation is consistent with recruitment of both naïve and memory B cells shown in other vaccine regimes for influenza, *Streptococcus pneumoniae*, etc. (26–28). The mutation rate range was broader after boost with the Vi-PS vaccine; however, only three mAbs were selected from the post-prime group, so median levels of mutations could not be compared between groups (fig. S6).

Vi polysaccharide antibodies exhibit heterogeneous avidity, and affinity maturation is not detected

To further characterize the binding and functional properties of Vi-specific mAbs, we first measured the avidity of each antibody to Vi PS antigen by BLI. Most mAb avidities were within a range of 10^3 to 10^5 (M^{-1} s^{-1}) for on-rate and 10^{-2} to 10^{-4} (s^{-1}) for off-rate. Overall, avidity measurements of the 53 mAbs that were positive for binding to the polymeric Vi PS antigen ranged from 10 μM to 500 pM (Fig. 3A), and Vi binding response magnitude showed moderate negative correlation with K_D ($r = -0.60$, $P < 0.0001$;

Fig. 3B), indicating a positive correlation with avidity. Only three antibodies were selected after prime with Vi-TT; these exhibited an avidity in the 1 μM range, similar to that of mAbs isolated from the same participant after boost (Fig. 3, C and D). Similarly, polyclonal sera collected after Vi-TT prime and Vi-PS boost showed no evidence of maturation (Fig. 3E). Therefore, within this sample set, there was no evidence of avidity maturation of Vi antibodies after repeat vaccination.

Vi vaccines induce convergent B cell responses with shared CDR3 characteristics

Evidence of interdonor B cell sequence convergence in the anti-Vi immune response allowed for successful selection of 53 Vi-specific mAbs. To further investigate the level of convergence, we examined the sequence characteristics, avidity, and epitope binning of each group of convergent mAbs. We compared heavy-chain sequences with the same V_H gene segment among the seven donors from whom Vi PS antigen binding antibodies were successfully isolated. Using a cutoff for heavy-chain CDR3 identity of 75% or greater (29), we identified five convergent groups of antibodies (G1 to G5). Each convergent group included antibodies from two or more individual donors, and six of seven donors were represented in at least one group, suggesting that convergent responses to the Vi PS antigen are common among vaccine recipients. Frequent use of V_H3–23 and Vκ3–11/ Vκ3–15 was observed in convergent groups (Fig. 4A). Within groups that shared V_H and V_L, all groups (G1 to G5) shared a high level of CDRH3 sequence similarity (ranging from 76.5 to 100%) (Fig. 4B). Cross-competition of antibodies within each group provided further evidence that antibodies showing evidence of convergence target similar sites on Vi PS (Fig. 4C). In nearly all instances, no blocking was observed with a convergent pair when the higher-avidity antibody bound after the lower-avidity antibody (an example being lower-avidity antibody AB-007972 versus higher-avidity AB-007981 in G2), whereas when the high avidity bound first, the secondary antibody was blocked. Competition seen between mAbs of different convergent groups, in addition to within groups, is consistent with overlapping epitopes among the Vi binding antibodies (fig. S7). Another possibility is that steric hindrance impedes binding to an adjacent but distinct site.

mAbs derived from Vi vaccination can target subdominant epitopes

To further resolve the epitope specificity of Vi mAbs derived by vaccination, we used a chemical modification to eliminate the immunodominant *O*-acetyl group at the C3 position and expose the polysaccharide backbone (Fig. 5A). The international standard (16/126) for Vi polysaccharide is 94.3% *O*-acetylated (30). Treatment with ammonium hydroxide (NH_4OH) was titrated to determine the concentration at which the *O*-acetyl groups are completely removed. At 1.0 M NH_4OH, the Vi PS antigen was completely de–*O*-acetylated (Fig. 5B and fig. S8), leaving a new C3 ^1H in its place. Of 53 mAbs, 47 exhibited C3 *O*-acetyl–dependent epitope specificities, including AB-008053, where binding to the Vi PS antigen was reduced by over 75% upon de–*O*-acetylation (Fig. 5, C and D, right). However, six mAbs (about 10% of the total pool) bound equally or with higher binding to de–*O*-acetylated Vi PS antigen as compared with native Vi PS antigen (Fig. 5D, left). Of those six mAbs, three displayed similar binding response and avidity to the native Vi PS and de–*O*-acetylated Vi PS antigens including AB-007988 (Fig. 5E and fig. S9A), indicating at least one subdominant, alternative epitope that is exposed (SEE) and independent of

the *O*-acetyl group. In addition, three mAbs bound with greater binding and avidity to the de–*O*-Vi PS antigen compared with the native Vi PS antigen including AB-008049 (Fig. 5F and fig. S9B), indicating at least one subdominant epitope that is occluded (SEO) by the C3 *O*-acetyl and is less solvent accessible.

Competition experiments with the anti–*O*-acetyl antibody AB-008053 further defined the epitope specificities of these six alternate specificity mAbs. After Vi PS antigen binding was saturated by AB-008053, the further increase in binding signal mediated by AB-007986 and AB-007981 indicates that these mAbs are specific for an epitope that is exposed (SEE) and non-adjacent to the C3 *O*-acetyl group (Fig. 6A). AB-007988, which bound with equal binding and avidity to the Vi PS and de–*O*-acetylated Vi PS antigens as well (Fig. 5E), was slightly blocked by AB-008053 in the competition assay (Fig. 6A). This suggests that AB-007988 binds an epitope adjacent to, but not dependent on, the C3 *O*-acetyl group and that perhaps steric hindrance by AB-008053 inhibited binding of AB-007988. This is confirmed by performing the competition in the reverse orientation where AB-007988 associated first, followed by AB-008053 (fig. S10A). All three mAbs that bound with higher binding and avidity to de–*O*-acetylated Vi PS compared with the native Vi PS antigen were blocked by the anti–*O*-acetyl mAb AB-008053 (Fig. 6B), confirming that the epitope specificity of these mAbs is shielded by the C3 *O*-acetyl group. Furthermore, a cross-competitive assessment of the six alternative epitope mAbs with each other confirmed that AB-007988 binds a distinct SEE epitope from the SEE epitope bound by AB-007986 and AB-007981 (Fig. 6C). In addition, there are two SEO epitopes, one that is only partially occluded by the *O*-acetyl group and was bound by AB-007973 and one that is completely occluded by the *O*-acetyl group and was bound by AB-008049 and AB-007985 (Fig. 6C). These experiments indicate that AB-007973 and AB-007988 bind overlapping but nonidentical epitopes, where the AB-007988 epitope is more solvent accessible and the AB-007973 epitope is slightly more occluded.

Vi antibodies mediate Fc-dependent effector functions

To identify the capacity of Vi binding antibodies to mediate Fc-dependent effector functions, we evaluated the Vi-specific mAbs in in vitro monocyte phagocytosis and complement deposition assays (figs. S11 and S12). Vi-specific mAbs mediated a broad range of ADMP and ADCD activity, with the mAbs specifically targeting an SEE epitope among the highest performers for both ADMP and ADCD (Fig. 7, A and B). On the contrary, mAbs that targeted an SEO epitope occluded by the C3 *O*-acetyl group performed poorly, likely because of the inaccessibility of the epitope (Fig. 7, A and B). Capacity to mediate ADMP was moderately associated with the capacity to mediate ADCD ($r = 0.51$, $P = 0.0001$; Fig. 7C).

The association rate (on-rate) of mAbs to Vi PS antigen had no impact on ADMP ($r = -0.01$, $P = 0.9452$; fig. S13A) or ADCD ($r = 0.26$, $P = 0.063$; fig. S13B); however, the dissociation rate (off-rate) of mAbs to Vi PS antigen was highly, negatively correlated (slower off-rate corresponds to higher function) with potency of ADMP ($r = -0.50$, $P = 0.0002$; Fig. 7D) and ADCD ($r = -0.74$, $P < 0.0001$; Fig. 7E). ADMP was weakly correlated with antibody avidity ($r = 0.38$, $P = 0.005$; Fig. 7D); however, ADCD was highly correlated with antibody

avidity ($r = -0.76$, $P < 0.0001$; Fig. 7E). In the current experimental setup, Vi mAbs with avidity lower than 500 nM did not mediate ADCD with Vi PS antigen–coated beads (Fig. 7E). These results indicate that antibodies targeting any epitope that is accessible, not merely the immunodominant C3 *O*- acetyl group, can mediate Fc effector function in a manner dependent on the antibody-antigen off-rate.

DISCUSSION

Recent analyses of immune correlates for typhoid Vi PS vaccines suggest that protection from typhoid is mediated by high titers of high-avidity IgG and IgA antibodies in combination with antibody-mediated innate immune cell function (12, 16, 17). Although Vi antibodies correlate with protection against typhoid, the properties of the vaccine-induced humoral immune response to Vi remain unknown. In this study, we isolated plasmablasts from individuals primed and boosted with Vi vaccines and evaluated the repertoire, avidity maturation, epitope specificity, and functionality of Vi mAbs. Our findings highlight that Vi vaccination elicits convergent, functional antibodies that target both immunodominant and subdominant Vi epitopes, and that ability to mediate Fc effector function is largely associated with antibody dissociation kinetics.

After both prime (Vi-TT) and boost (Vi-PS), the predominant antibody subclass expressed by B cells was IgG1, the most common antibody subclass in serum. A Vi-PS boost resulted in an increase in IgG2-expressing plasmablasts likely from new marginal zone or B1 B cells induced directly by the unconjugated, T-independent polysaccharide. Previously, it has been reported that polysaccharides are likely to induce an IgG2 response (31–33), which has also been observed for the Vi-PS vaccine (16). The number of IgG3 sequences detected in this study is lower than would be expected based on antibody data (16). Responses evaluated after Vi-PS would include boosting of existing memory B cells induced by the conjugate prime and newly activated B cell clones, consistent with the broad range of somatic hypermutations in the antibody variable regions (range, 2 to 47). Therefore, although the prime-boost strategy allows for a robust humoral response to be generated toward Vi, this strategy does make it difficult to determine whether the Vi-PS vaccine response evaluated here is a typical response for Vi-PS immunization. The prime-boost strategy does allow the direct comparison of repertoires within the same individual. Here, we highlighted four of the IgHV genes for which a difference in frequency was observed between the Vi-TT and Vi-PS vaccines. IgHV3–23 is one of the most commonly observed genes (34), and antibodies using this region have previously been described to recognize other polysaccharides such as the *H. influenzae* type b (Hib) polysaccharide (35). Allelic variances in IgHV3–23 were also shown to influence antibody binding and effector function toward this antigen (35).

Using the selection criteria of convergence, persistence, and expansion, we isolated 96 mAbs, of which 52 were positive for binding the 94.3% *O*-acetylated Vi PS antigen, with 1 additional binding to de–*O*-acetylated Vi PS antigen only, for a total of 53. Only 2 mAbs bound to TT; therefore, either the remaining 41 mAbs have an unidentified antigen specificity or the affinity of these antibodies for Vi is too low to measure by BLI. The mAbs that had measurable binding responses for Vi exhibited a range of K_D from around 10 μM to around 500 pM; however, the measurement of K_D is representative of avidity not

true affinity due to the size of the Vi polymer and binding by full IgG molecules. Future studies to measure affinity would require digestion of mAbs into single Fab fragments and synthesizing the Vi minimal epitope, shown to be a hexamer (36), rather than using the native Vi PS antigen, which contains greater than 10,000 U (37). Therefore, the measured avidity must be higher than the true affinity of these mAbs, which are likely to be near the lower range of 10 μM, similar to most other isolated polysaccharide mAbs against other pathogens (38, 39). There was no evidence of affinity maturation at the population level, also reported in a CHIM study after Vi vaccination (16), and there is unlikely to be affinity maturation occurring on the individual level within a clonal lineage. Here, we selected one representative mAb from each expanded or persistent family; therefore, the changes within clonal lineages cannot be examined. However, these results are not unexpected as boosting with unconjugated Vi polysaccharide, a T cell–independent antigen, is unlikely to drive affinity maturation (40, 41).

Naturally occurring *S.* Typhi isolates exhibit Vi PS where 60 to 90% of monomers are *O*-acetylated (21), and currently licensed Vi-based vaccines require a threshold of >52% *O*-acetylation (23). Previous studies have established that vaccination with highly *O*-acetylated Vi still induces low-level polyclonal antibody responses to other unknown epitopes on the polysaccharide backbone (20, 22), but the functional relevance of these subdominant responses, if any, has not been described. Here, we show that around 10% of the selected Vi PS plasmablast pool are specific for subdominant, non–*O*-acetyl epitopes and that these antibodies appear after prime, after boost, and in more than half of the donors, indicating that these responses are common. However, whether these antibodies arise because of new epitope exposure via Vi conjugation to TT, which has been shown to change the conformation and flexibility of other vaccine antigens, is unknown (42, 43). We show that although the *O*-acetyl group is the immunodominant epitope, antibodies arise that target at least four distinct, alternative epitopes, two that are subdominant but solvent-exposed (SEE) and two that are completely or partially occluded from the surface (SEO). The level of convergence and competition between Vi binding mAbs suggests that likely only a small number of overlapping and adjacent epitopes exist on the Vi PS. Possible epitope specificities are presumably limited because of the nature of the antigen as a homopolymer with a small repeating monomer. Epitope mapping using additional site-directed modifications of the polysaccharide would define the epitope specificities of these mAbs and determine whether the mAb binding sites are identical or are competing by steric hindrance due to recognition of overlapping epitopes.

We observed that mAbs targeting the subdominant exposed epitopes were among the highest performers for ADMP and ADCD, indicating that responses toward subdominant regions may be functional in preventing or controlling typhoid fever. However, mAbs targeting the subdominant epitope occluded by *O*-acetyl groups performed poorly for ADMP and ADCD likely because of the inaccessibility of the epitope for binding. Partial de–*O*-acetylation of Vi (~45 to 60%) increased immunogenicity of Vi (20) by increasing the flexibility of the polysaccharide backbone (22), and de–*O*-acetylation also exposes new epitopes. We found that antibodies to these exposed subdominant epitopes (SEE) mediated potent antibody-dependent Fc effector functions, providing rationale to test the role of these antibodies in protection against or control of *S.* Typhi infection.

Properties that influence antibody-mediated effector functions include epitope-paratope interactions and Fc-FcR interactions. We found that potency of monocyte phagocytosis and complement deposition were significantly correlated with antibody off-rate, but not with on-rate, consistent with a prior study (44) and distinct from neutralization, which was linked to association rates (45, 46).

This study has several limitations. The focus of the antibody kinetics and functional analyses is limited to Vi IgG1 mAbs, without analysis of additional isotypes and subclasses. Given that a large proportion of antibodies mounted against Vi PS after vaccination with Vi-PS are of the IgG2 subclass and that allosteric changes can influence binding kinetics (47, 48), further studies with the natural antibody isotype and subclass are needed. In addition, because Vi PS IgA correlated with protection in a CHIM to study typhoid (16), an assessment of the IgA^+ plasmablast pool and characterization of IgA specificity and function is warranted. Other limitations of this study include the small number of participants from which plasmablasts were isolated ($n = 8$) and the small number of prime time point antibodies and prime-boost paired samples to assess affinity maturation. However, the presence of high-avidity antibodies after the boost and the finding that function is dependent on maturation of the antibody off-rate provides evidence that boosting may elicit more kinetically and functionally mature antibodies. High-avidity antibodies with antibody Fc effector functions correspond with protection from disease in a typhoid CHIM (16, 17). Serum bactericidal activity did not correlate with protection; however, the role of complement activation as part of a polyfunctional response is not fully understood (49). There is room to improve on the efficacy of the Vi-TT vaccine regimen to move from 82 and 85% efficacy in Nepal and Bangladesh, respectively (13, 50), to an ideal of 100% in diverse populations, including immunocompromised individuals. The results from this current study provide rationale to test whether a boost immunization provides better protection than a single-dose vaccination alone to achieve maximum efficacy in all populations. Although the Vi-PS boost in this study enriched Vi-specific plasmablasts to study Vi-specific immunity, likely a boost with Vi-TT would provide the most robust affinity maturation while maintaining the critical memory B cell pool.

In summary, we identified that antibodies to both dominant and subdominant epitopes mediated in vitro phagocytosis and complement deposition. Moreover, functional responses correlated with antibody dissociation rate from Vi. Broadening the antibody epitope targeting and Fc-mediated effector functions for *S.* Typhi Vi is a promising strategy for improving Vi vaccine regimens with higher efficacy in different populations.

MATERIALS AND METHODS

Study design

The objective of our study was to characterize the human antibody response induced by a prime-boost vaccination strategy against *S.* Typhi virulence factor Vi polysaccharide and to test the hypothesis that diverse and subdominant epitope specificities could mediate antibody Fc effector functions. We sorted and sequenced plasmablasts from vaccinated individuals ($n = 8$) after prime and boost and selected a pool ($n = 96$) of sequences to express as mAbs. We examined the convergence in B cell responses by examining V gene usage and CDR3

characteristics between vaccinees. Using different forms of the Vi polysaccharide antigen (*O*-acetylated and de–*O*-acetylated), we defined the specificity of vaccine-derived mAbs and the avidity maturation of these antibodies after prime and boost. Last, we investigated the ability of these antibodies to mediate Fc effector functions in cell-based assays and established the relationship between Fc function, specificity, and avidity.

Sample collection

We analyzed 12 participants, from a completed clinical trial (12), who were primed with a Vi-TT vaccine (Typbar TCV, Bharat Biotech, Hyderabad, India). Of the 10 participants who completed the study, 40% were female, and the mean age of participants was 39 ± 12 years (±SD). PBMCs were acquired before immunization and 7 days after immunization. Serum was available before immunization and 28 days after immunization with Vi-TT. Five participants were orally challenged with *S.* Typhi 28 days after receiving the initial immunization. Challenge did not increase antibody responses toward Vi (51). All participants received a boost with Vi-PS (TYPHIM Vi, Sanofi Pasteur, Lyon, France). The Vi-PS boost was administered between 19 and 23 months after the initial Vi-TT immunization. PBMCs were acquired before immunization and 7 days after immunization, and serum was available 28 days after immunization with Vi-PS.

All volunteers provided written informed consent before enrollment. The study protocol was approved by the sponsor (University of Oxford), the South Central Oxford A Ethics Committee (14/SC/1427), and the Medicines and Healthcare Products Regulatory Agency (Eudract 2014–002978-36).

Single-cell BCR sequencing

PBMC samples were selected for BCR sequencing based on sample availability. Single $CD62L^-$ or $CD62L^+$ plasmablasts ($CD19^+$ $CD20^-CD38^{hi}CD27^+CD3^-CD14^-IgA^-IgM^-IgD^-$) were individually sorted into wells of 384-well plates using FACSAria Fusion (BD Biosciences, USA). Generation of barcoded complementary DNA (cDNA), polymerase chain reaction (PCR) amplification, and sequencing of IgG genes were performed as described previously (52) with the following modifications: Biotinylated Oligo(dT) and RT maxima H− (Fisher Scientific Company) were used for reverse transcription, cDNA was extracted using Streptavidin C1 beads (Life Technologies), and DNA concentrations were determined using quantitative PCR (KAPA SYBR FAST qPCR Kit for Titanium, Kapa Biosystems). V(D)J assignment and mutation identification were performed using a variant of SoDA (53).

Plasmid generation and expression of mAbs

Variable heavy- and light-chain DNA sequences were synthesized and cloned into the respective human IgG1 heavy-chain or endogenous light-chain expression plasmids (LakePharma Inc.). The matched pair of heavy- and light-chain plasmids was transiently cotransfected into human embryonic kidney (HEK)–293 cells. Antibody supernatants were harvested 7 days after transfection, purified using protein A affinity chromatography, and filtered through a 0.2-μm filter. The final elution buffer for all antibodies was 100 mM Hepes, 100 mM NaCl, and 50 mM NaOAc (pH 6.0). Nomenclature for isolated antibodies

includes AB-00 followed by a four-number string. For graphing purposes, AB-00 may be omitted.

Vi-biotinylation and bead coupling

The International Standard for *Citrobacter freundii* Vi PS (NIBSC 12/244) with a 94.3% *O*-acetylation level was biotinylated by Expedeon (Cambridge, UK). A biotin binding assay (HABA) was carried out to confirm successful biotinylation. It was estimated that each Vi PS molecule contained 14 biotins after the modification procedure.

Phycoerythrin (PE)–neutravidin beads (Life Technologies) were coated with Vi by incubating 2.5 μg of biotinylated Vi with 10 μl of beads for a duration of 2 hours at 37°C. Beads were washed twice with 1 ml of phosphate-buffered saline (PBS) and 5% bovine serum albumin (BSA; microcentrifuged at 13,000 rpm for 2 min) and taken up in 1 ml of RPMI for each 10 μl of original bead volume. Coupled beads were used for functional measurements.

Biolayer interferometry

BLI measurements were collected with ForteBio Octet RED384 instruments. Kinetics of Vi mAbs binding to Vi PS or de–*O*-Vi PS were analyzed by BLI as previously described (16) with modifications. Briefly, native Vi PS antigen or de–*O*-acetylated Vi PS (5 μg/ml) was immobilized to ForteBio aminopropylsilane (APS) biosensors via hydrophobic interaction, followed by washing sensors with 10X Kinetics Buffer (10X KB) (ForteBio, USA) to coat unoccupied sensor area and minimize nonspecific interactions. A baseline was established in 1X KB, and then Vi-loaded sensors were dipped into wells containing Vi mAbs (in 1X KB) to monitor mAb association. Dissociation was monitored by dipping Vi mAb–associated sensors back into the 1X KB wells used to collect the baseline time course. Each mAb was titrated seven places starting at 10 μg/ml, twofold. Parallel blank sensors that were also washed in 10X KB and dipped in Vi mAbs were used to subtract out nonspecific interactions. At least four of seven reference subtracted binding curves were globally fit using ForteBio Data Analysis 10.0 software to determine antibody binding response (nm), on-rate (k_a), off-rate (k_d), and observed avidity (K_D). Fitting window was adjusted to minimize effects of upward drift/rebinding in the dissociation phase.

Competition experiments were conducted by immobilizing Vi PS antigen (5 μg/ml) to APS biosensors at very low density (0.01-nm loading threshold). After washing with 10X KB, sensors were dipped into wells containing antibody 1 at 10 μg/ml (in 1X KB) to bind to complete saturation. Sensors were then dipped into wells containing a second Vi mAb at 10 μg/ml (in 1X KB). Last, sensors were dipped back into wells containing 1X KB to allow dissociation. No blocking is described as an increase in binding signal upon dipping into antibody 2. Blocking is described as a flat line or decrease in binding signal upon dipping into antibody 2.

Enzyme-linked immunosorbent assay

Serum Vi IgG antibodies were quantified using the VaccZyme Human Anti-S typhi Vi IgG ELISA Kit (VaccZyme, Birmingham, UK). Specificity of mAbs was determined using the

VaccZyme Human Anti-S typhi Vi IgG ELISA Kit and a tetanus toxoid IgG enzyme-linked immunosorbent assay (ELISA) kit (VaccZyme, Birmingham, UK). Total serum antibody data were published previously as part of the main study (12).

Total serum avidity was measured using a modified Vi ELISA in combination with NaSCN. Nunc MaxiSorp U-bottom plates were coated using streptavidin (Thermo Scientific, 43–4301) at 2 μg/ml overnight at 37°C, followed by a 1-hour incubation with biotinylated Vi at 2 μg/ml for 1 hour at room temperature (RT). The plate was blocked with PBS and 1% BSA for 1 hour at RT. Serum dilutions were chosen to ensure that the binding of the samples was in the linear phase of their titration curve. Samples from the same person were tested on one plate. Serum samples, diluted in PBS, 1% BSA, and 30% Brij 35, were incubated for 1 hour at 37°C and incubated with several concentrations of NaSCN (5, 1, 0.5, 0.25, 0.125, and 0 M) for 15 min at RT. IgG antibodies bound to the plate were detected with Mouse monoclonal Anti-Human IgG Fc (Alkaline Phosphatase) (Abcam, ab99764) and incubated for 1 hour at 37°C. Residual binding was detected using the combination 4-Nitrophenyl Phosphate (pNPP) Liquid Substrate System (Sigma-Aldrich, N7653) and a 3 M NaOH stop solution. The avidity index of each sample was calculated as a percentage of residual binding: x M/(0 M − 5 M), where x was a concentration of NaSCN in between 0 and 5 M.

De–*O*-acetylation of Vi polysaccharide

Vi PS was de–*O*-acetylated using a method by Hitri *et al.* (22) adapted from the method described by Szu *et al.* (20). Briefly, one vial of the International Standard for Vi PS NIBSC 12/244 was rehydrated in water (1 mg/ml) and was diluted in airtight tubes with 10 M ammonium hydroxide (NH_4OH) to a final concentration of 50, 150, 300, 500, and 700 mM for partial de–*O*-acetylation and 1 or 1.5 M NH_4OH for full de–*O*-acetylation. Samples were capped and incubated at 37°C for 18 hours. Solvent was evaporated, and the de–*O*-acetylated Vi PS (de–*O*-Vi PS) pellet was rehydrated in water overnight before use. For nuclear magnetic resonance (NMR) experiments, Vi PS was rehydrated before and after de–*O*-acetylation with deuterated water (D_2O).

NMR spectroscopy

NMR was performed on a Bruker 16.4 Tesla spectrometer (Bruker, USA) with a BBO RT probe. Before measurement, individual samples were exchanged/lyophilized two times, each time resuspending the polysaccharide in 600 μl of D_2O. The *O*-acetylation level of control (untreated) and 0.05, 0.15, 0.3, 0.7, 1.0, and 1.5 M NH_4OH-treated Vi PS solutions was investigated by two-dimensional ^{1}H-^{13}C heteronuclear single quantum coherence (HSQC) spectroscopy analyses. Quantification of the *N*- and *O*-acetyl signals were possible in the ^{1}H-^{13}C HSQC because they are well resolved. The intensity of the *N*- and *O*-acetyl crosspeaks [~^{1}H at 1.9 parts per million (ppm)] was used to determine the ratio of *O*- to *N*-acetylation. ^{1}H-^{13}C HSQC two-dimensional experiments were performed using the hsqccetgpsisp2.2 pulse sequence, with a 1J(CH) coupling constant of 145 Hz. Processing was done using TopSpin 4.0.1 (Bruker, USA).

Antibody-dependent monocyte phagocytosis

The capacity of mAbs (concentration, 1 μg/ml) to mediate ADMP was performed as previously described in THP1 cells (54). The phagocytic score for each sample was determined by multiplying the percent of bead-positive cells with the GMFI (geometric mean fluorescence intensity) of the bead-positive cells. Debris and doublets were removed by manual gating before carrying out these calculations.

Antibody-dependent complement deposition

ADCD was performed as previously described (55), with the following modifications. mAbs (1 μg/ml) were incubated with antigen-coated beads for 15 min at 37°C and then with complement (Low-T ox Guinea Pig Complement, Cedarlane, CL4051) for 15 min at 37°C. The plate was centrifuged at 1000*g* for 3 min at 4°C; plates were washed with PBS (200 μl per well) with 15 mM EDTA and incubated with fluorescein isothiocyanate–conjugated Goat IgG Fraction to Guinea Pig Complement C3 (MP Biomedicals, 855385) for 20 min, and the wash step was repeated.

Complement deposition was assessed by determining the GMFI of anti-C3 intensity on PE-positive beads (BD LSRFortessa X-20). Doublets and debris were removed by manual gating before carrying out these calculations.

Quantification and statistics

The sequence similarity index of CDRH3 sequences in convergent antibody groups was calculated by EMBOSS Needle using pairwise alignment and BLOSUM62 (Blocks Substitution Matrix 62) with residue-specific and hydrophilic gap penalties (open gap penalty, 10; extended gap penalty, 0.5). For the selection of antibodies for protein expression based on convergence, the BLOSUM62 similarity was calculated for pairs of antibodies from different donors. Putative convergent antibodies were required to have greater similarity than that observed between pairs of unrelated antibodies (56).

CDR3 lengths were examined using the Shapiro-Wilk normality test R software (version 3.6.1). The relationship between CD62L expression on plasmablasts and antibody Vi specificity was evaluated by Fisher’s exact test, and the relationship between the functional and kinetic measurements was evaluated by Spearman correlation analysis in SAS software (version 9.4 of the SAS System, copyright 2002–2012 by SAS Institute Inc., Cary, NC, USA).

Supplementary Material

Refer to Web version on PubMed Central for supplementary material.

Acknowledgments:

We offer our sincerest thanks to our volunteers for participating in the study; the Oxford Vaccine Group Typhoid Study Team, particularly E. Plested for project managing the study, S. Milca for recruitment efforts, and L. Khan for assisting with the organization of the study; D. Lalloo (chair) and members of the Data Safety and Monitoring Committee for providing study oversight and guidance; Bharat Biotech International Limited for supplying the investigational vaccine (Typbar TCV); M. M. Levine and the University of Maryland for provision of the original *S.* Typhi Quailes challenge strain; the Wellcome Trust for funding the development of the typhoid challenge model;

the Division of Bacteriology from the National Institute of Biological Standards and Control (NIBSC) for provision of the 12/244 International Standard for Vi polysaccharide antigen and guidance on the de-*O*-acetylation process and NMR; members of the Center for Human Systems Immunology, including S. Mudrak for GH-VAP program management support and additional laboratory members J. Li, D. Goodman, D. Tenney, and R. Thomas for training and specimen management; and the Duke University NMR Spectroscopy Center for use of their instrumentation.

Funding:

This study was supported by the Bill and Melinda Gates Foundation (OPP1084259 and OPP1188863 to A.J.P.), a grant for the Antibody Dynamics platform of the Global Health-Vaccine Accelerator Platforms (GH-VAP) from the Bill and Melinda Gates Foundation (OPP1151372 and OPP1210938 to G.D.T.), and the NIHR Oxford Biomedical Research Centre. Additional support was provided by the Dean's Graduate Fellowship, Duke University.

Data and materials availability:

All data needed to evaluate the conclusions in the paper are present in the paper or the Supplementary Materials.

REFERENCES AND NOTES

1. Plotkin SA, Correlates of protection induced by vaccination. Clin. Vaccine Immunol 17, 1055–1065 (2010). [PubMed: 20463105]
2. Käyhty H, Peltola H, Karanko V, Mäkelä PH, The protective level of serum antibodies to the capsular polysaccharide of Haemophilus influenzae type b. J. Infect. Dis 147, 1100 (1983). [PubMed: 6602191]
3. Frasch CE, Borrow R, Donnelly J, Bactericidal antibody is the immunologic surrogate of protection against meningococcal disease. Vaccine 27 (Suppl. 2), B112–B116 (2009). [PubMed: 19464093]
4. Maciejewski S, Ruckwardt TJ, Morabito KM, Foreman BM, Burgomaster KE, Gordon DN, Pelc RS, DeMaso CR, Ko SY, Fisher BE, Yang ES, Nair D, Foulds KE, Todd JP, Kong WP, Roy V, Aleshnick M, Speer SD, Bourne N, Barrett AD, Nason MC, Roederer M, Gaudinski MR, Chen GL, Dowd KA, Ledgerwood JE, Alter G, Mascola JR, Graham BS, Pierson TC, Distinct neutralizing antibody correlates of protection among related Zika virus vaccines identify a role for antibody quality. Sci. Transl. Med 12, eaaw9066 (2020).
5. Pittala S, Bagley K, Schwartz JA, Brown EP, Weiner JA, Prado IJ, Zhang W, Xu R, Ota-Setlik A, Pal R, Shen X, Beck C, Ferrari G, Lewis GK, LaBranche CC, Montefiori DC, Tomaras GD, Alter G, Roederer M, Fouts TR, Ackerman ME, Bailey-Kellogg C, Antibody Fab-Fc properties outperform titer in predictive models of SIV vaccine-induced protection. Mol. Syst. Biol 15, e8747 (2019).
6. Feng J, Gulati U, Zhang X, Keitel WA, Thompson DM, James JA, Thompson LF, Air GM, Antibody quantity versus quality after influenza vaccination. Vaccine 27, 6358–6362 (2009). [PubMed: 19840673]
7. Kazmin D, Nakaya HI, Lee EK, Johnson MJ, van der Most R, van den Berg RA, Ballou WR, Jongert E, Wille-Reece U, Ockenhouse C, Aderem A, Zak DE, Sadoff J, Hendriks J, Wrammert J, Ahmed R, Pulendran B, Systems analysis of protective immune responses to RTS,S malaria vaccination in humans. Proc. Natl. Acad. Sci. U.S.A 114, 2425–2430 (2017). [PubMed: 28193898]
8. Mohan VK, Varanasi V, Singh A, Pasetti MF, Levine MM, Venkatesan R, Ella KM, Safety and immunogenicity of a Vi polysaccharide-tetanus toxoid conjugate vaccine (Typbar-TCV) in healthy infants, children, and adults in typhoid endemic areas: A multicenter, 2-cohort, open-label, double-blind, randomized controlled phase 3 study. Clin. Infect. Dis 61, 393–402 (2015). [PubMed: 25870324]
9. GBD 2017 Typhoid and Paratyphoid Collaborators, The global burden of typhoid and paratyphoid fevers: A systematic analysis for the Global Burden of Disease Study 2017. Lancet Infect. Dis 19, 369–381 (2019). [PubMed: 30792131]
10. Wong VK, Baker S, Pickard DJ, Parkhill J, Page AJ, Feasey NA, Kingsley RA, Thomson NR, Keane JA, Weill FX, Edwards DJ, Hawkey J, Harris SR, Mather AE, Cain AK, Hadfield J, Hart PJ, Thieu NT, Klemm EJ, Glinos DA, Breiman RF, Watson CH, Kariuki S, Gordon MA, Heyderman RS, Okoro C, Jacobs J, Lunguya O, Edmunds WJ, Msefula C, Chabalgoity JA, Kama M, Jenkins

K, Dutta S, Marks F, Campos J, Thompson C, Obaro S, MacLennan CA, Dolecek C, Keddy KH, Smith AM, Parry CM, Karkey A, Mulholland EK, Campbell JI, Dongol S, Basnyat B, Dufour M, Bandaranayake D, Naseri TT, Singh SP, Hatta M, Newton P, Onsare RS, Isaia L, Dance D, Davong V, Thwaites G, Wijedoru L, Crump JA, De Pinna E, Nair S, Nilles EJ, Thanh DP, Turner P, Soeng S, Valcanis M, Powling J, Dimovski K, Hogg G, Farrar J, Holt KE, Dougan G, Phylogeographical analysis of the dominant multidrug-resistant H58 clade of Salmonella Typhi identifies inter- and intracontinental transmission events. Nat. Genet 47, 632–639 (2015). [PubMed: 25961941]

11. Klemm EJ, Shakoor S, Page AJ, Qamar FN, Judge K, Saeed DK, Wong VK, Dallman TJ, Nair S, Baker S, Shaheen G, Qureshi S, Yousafzai MT, Saleem MK, Hasan Z, Dougan G, Hasan R, Emergence of an extensively drug-resistant Salmonella enterica Serovar typhi clone harboring a promiscuous plasmid encoding resistance to fluoroquinolones and third-generation cephalosporins. MBio 9, e00105–18 (2018).
12. Jin C, Gibani MM, Moore M, Juel HB, Jones E, Meiring J, Harris V, Gardner J, Nebykova A, Kerridge SA, Hill J, Thomaides-Brears H, Blohmke CJ, Yu LM, Angus B, Pollard AJ, Efficacy and immunogenicity of a Vi-tetanus toxoid conjugate vaccine in the prevention of typhoid fever using a controlled human infection model of Salmonella Typhi: A randomised controlled, phase 2b trial. Lancet 390, 2472–2480 (2017). [PubMed: 28965718]
13. Shakya M, Colin-Jones R, Theiss-Nyland K, Voysey M, Pant D, Smith N, Liu X, Tonks S, Mazur O, Farooq YG, Clarke J, Hill J, Adhikari A, Dongol S, Karkey A, Bajracharya B, Kelly S, Gurung M, Baker S, Neuzil KM, Shrestha S, Basnyat B, Pollard AJ; TyVAC Nepal Study Team, Phase 3 efficacy analysis of a typhoid conjugate vaccine trial in nepal. N. Engl. J. Med 381, 2209–2218 (2019). [PubMed: 31800986]
14. Klugman KP, Koornhof HJ, Robbins JB, Le Cam NN, Immunogenicity, efficacy and serological correlate of protection of Salmonella typhi Vi capsular polysaccharide vaccine three years after immunization. Vaccine 14, 435–438 (1996). [PubMed: 8735556]
15. Szu SC, Klugman KP, Hunt S, Re-examination of immune response and estimation of anti-Vi IgG protective threshold against typhoid fever-based on the efficacy trial of Vi conjugate in young children. Vaccine 32, 2359–2363 (2014). [PubMed: 24630869]
16. Dahora LC, Jin C, Spreng RL, Feely F, Mathura R, Seaton KE, Zhang L, Hill J, Jones E, Alam SM, Dennison SM, Pollard AJ, Tomaras GD, IgA and IgG1 specific to Vi polysaccharide of *Salmonella* typhi correlate with protection status in a typhoid fever controlled human infection model. Front. Immunol 10, 2582 (2019). [PubMed: 31781100]
17. Jin C, Hill J, Gunn BM, Yu WH, Dahora LC, Jones E, Johnson M, Gibani MM, Spreng RL, Alam SM, Nebykova A, Juel HB, Dennison SM, Seaton KE, Fallon JK, Tomaras GD, Alter G, Pollard AJ, Vi-specific serological correlates of protection for typhoid fever. J. Exp. Med 218, (2021).
18. Dougan G, Baker S, *Salmonella enterica* Serovar Typhi and the pathogenesis of typhoid fever. Annu. Rev. Microbiol 68, 317–336 (2014). [PubMed: 25208300]
19. Wangdi T, Lee CY, Spees AM, Yu C, Kingsbury DD, Winter SE, Hastey CJ, Wilson RP, Heinrich V, Baumler AJ, The Vi capsular polysaccharide enables Salmonella enterica serovar typhi to evade microbe-guided neutrophil chemotaxis. PLOS Pathog. 10, e1004306 (2014).
20. Szu SC, Li XR, Stone AL, Robbins JB, Relation between structure and immunologic properties of the Vi capsular polysaccharide. Infect. Immun 59, 4555–4561 (1991). [PubMed: 1937814]
21. Berti F, De Ricco R, Rappuoli R, Role of O-acetylation in the immunogenicity of bacterial polysaccharide vaccines. Molecules 23, 1340 (2018). [PubMed: 29865239]
22. Hitri K, Kuttel MM, De Benedetto G, Lockyer K, Gao F, Hansal P, Rudd TR, Beamish E, Rijpkema S, Ravenscroft N, Bolgiano B, O-acetylation of typhoid capsular polysaccharide confers polysaccharide rigidity and immunodominance by masking additional epitopes. Vaccine 37, 3866–3875 (2019). [PubMed: 31160100]
23. Guidelines on the quality, safety and efficacy of typhoid conjugate vaccines. WHO Tech. Rep. Ser 987, 101–157 (2014).
24. Szewczyk B, Taylor A, Diversity of Vi-related antigens in the microcapsule of Salmonella typhi. Infect. Immun 30, 661–667 (1980). [PubMed: 6164644]
25. Qadri A, Ghosh S, Talwar GP, Monoclonal antibodies against two discrete determinants on Vi capsular polysaccharide. J. Immunoassay 11, 235–250 (1990). [PubMed: 1693381]

26. Henry C, Zheng NY, Huang M, Cabanov A, Rojas KT, Kaur K, Andrews SF, Palm AE, Chen YQ, Li Y, Hoskova K, Utset HA, Vieira MC, Wrammert J, Ahmed R, Holden-Wiltse J, Topham DJ, Treanor JJ, Ertl HC, Schmader KE, Cobey S, Krammer F, Hensley SE, Greenberg H, He XS, Wilson PC, Influenza virus vaccination elicits poorly adapted B cell responses in elderly individuals. Cell Host Microbe 25, 357–366.e6 (2019).
27. Zhou J, Lottenbach KR, Barenkamp SJ, Reason DC, Somatic hypermutation and diverse immunoglobulin gene usage in the human antibody response to the capsular polysaccharide of Streptococcus pneumoniae type 6B. Infect. Immun 72, 3505–3514 (2004). [PubMed: 15155658]
28. Chen Z, Cox KS, Tang A, Roman J, Fink M, Kaufhold RM, Guan L, Xie A, Boddicker MA, McGuinness D, Xiao X, Li H, Skinner JM, Verch T, Retzlaff M, Vora KA, Human monoclonal antibodies isolated from a primary pneumococcal conjugate vaccinee demonstrates the expansion of an antigen-driven hypermutated memory B cell response. BMC Infect. Dis 18, 613 (2018). [PubMed: 30509199]
29. Ehrhardt SA, Zehner M, Krahling V, Cohen-Dvashi H, Kreer C, Elad N, Gruell H, Ercanoglu MS, Schommers P, Gieselmann L, Eggeling R, Dahlke C, Wolf T, Pfeifer N, Addo MM, Diskin R, Becker S, Klein F, Polyclonal and convergent antibody response to Ebola virus vaccine rVSV-ZEBOV. Nat. Med 25, 1589–1600 (2019). [PubMed: 31591605]
30. Gao F, Swann C, Rigsby P, Rijpkema S, Lockyer K, Logan A, Bolgiano B; Vi IS Working Group, Evaluation of two WHO First International Standards for Vi polysaccharide from Citrobacter freundii and Salmonella enterica subspecies enterica serovar Typhi. Biologicals 57, 34–45 (2019). [PubMed: 30502020]
31. Hjelholt A, Christiansen G, Sorensen US, Birkelund S, IgG subclass profiles in normal human sera of antibodies specific to five kinds of microbial antigens. Pathog. Dis 67, 206–213 (2013). [PubMed: 23620184]
32. Barrett DJ, Ayoub EM, IgG2 subclass restriction of antibody to pneumococcal polysaccharides. Clin. Exp. Immunol 63, 127–134 (1986). [PubMed: 3955880]
33. Vidarsson G, Dekkers G, Rispens T, IgG subclasses and allotypes: From structure to effector functions. Front. Immunol 5, 520 (2014). [PubMed: 25368619]
34. Briney B, Inderbitzin A, Joyce C, Burton DR, Commonality despite exceptional diversity in the baseline human antibody repertoire. Nature 566, 393–397 (2019). [PubMed: 30664748]
35. Liu L, Lucas AH, IGH V3–23*01 and its allele V3–23*03 differ in their capacity to form the canonical human antibody combining site specific for the capsular polysaccharide of Haemophilus influenzae type b. Immunogenetics 55, 336–338 (2003). [PubMed: 12845501]
36. Zhang G-L, Wei M-M, Song C, Ma Y-F, Zheng X-J, Xiong D-C, Ye X-S, Chemical synthesis and biological evaluation of penta- to octa- saccharide fragments of Vi polysaccharide from Salmonella typhi. Org. Chem. Front 5, 2179–2188 (2018).
37. Szu SC, Li XR, Schneerson R, Vickers JH, Bryla D, Robbins JB, Comparative immunogenicities of Vi polysaccharide-protein conjugates composed of cholera toxin or its B subunit as a carrier bound to high- or lower-molecular-weight Vi. Infect. Immun 57, 3823–3827 (1989). [PubMed: 2807549]
38. Harris SL, Fernsten P, Thermodynamics and density of binding of a panel of antibodies to high-molecular-weight capsular polysaccharides. Clin. Vaccine Immunol 16, 37–42 (2009). [PubMed: 19005020]
39. Cygler M, Rose DR, Bundle DR, Recognition of a cell-surface oligosaccharide of pathogenic *Salmonella* by an antibody Fab fragment. Science 253, 442–445 (1991). [PubMed: 1713710]
40. Rijkers GT, Sanders EA, Breukels MA, Zegers BJ, Infant B cell responses to polysaccharide determinants. Vaccine 16, 1396–1400 (1998). [PubMed: 9711778]
41. Weintraub A, Immunology of bacterial polysaccharide antigens. Carbohydr. Res 338, 2539–2547 (2003). [PubMed: 14670715]
42. Laferriere CA, Sood RK, de Muys JM, Michon F, Jennings HJ, Streptococcus pneumoniae type 14 polysaccharide-conjugate vaccines: Length stabilization of opsonophagocytic conformational polysaccharide epitopes. Infect. Immun 66, 2441–2446 (1998). [PubMed: 9596700]

43. Abdelhameed AS, Morris GA, Almutairi F, Adams GG, Duvivier P, Conrath K, Harding SE, Solution conformation and flexibility of capsular polysaccharides from Neisseria meningitidis and glycoconjugates with the tetanus toxoid protein. Sci. Rep 6, 35588 (2016).
44. Macura N, Zhang T, Casadevall A, Dependence of macrophage phagocytic efficacy on antibody concentration. Infect. Immun 75, 1904–1915 (2007). [PubMed: 17283107]
45. Steckbeck JD, Orlov I, Chow A, Grieser H, Miller K, Bruno J, Robinson JE, Montelaro RC, Cole KS, Kinetic rates of antibody binding correlate with neutralization sensitivity of variant simian immunodeficiency virus strains. J. Virol 79, 12311–12320 (2005).
46. Bates JT, Keefer CJ, Utley TJ, Correia BE, Schief WR, Crowe JE Jr., Reversion of somatic mutations of the respiratory syncytial virus-specific human monoclonal antibody Fab19 reveal a direct relationship between association rate and neutralizing potency. J. Immunol 190, 3732–3739 (2013). [PubMed: 23455501]
47. Zhao J, Nussinov R, Ma B, Antigen binding allosterically promotes Fc receptor recognition. MAbs 11, 58–74 (2019). [PubMed: 30212263]
48. Su CT, Lua WH, Ling WL, Gan SK, Allosteric effects between the antibody constant and variable regions: A study of IgA Fc mutations on antigen binding. Antibodies 7, 20 (2018). [PubMed: 31544872]
49. Jones E, Jin C, Stockdale L, Dold C, Pollard AJ, Hill J, A Salmonella Typhi controlled human infection study for assessing correlation between bactericidal antibodies and protection against infection induced by typhoid vaccination. Microorganisms 9, 1394 (2021). [PubMed: 34203328]
50. Qadri F, Khanam F, Liu X, Theiss-Nyland K, Biswas PK, Bhuiyan AI, Ahmmed F, Colin-Jones R, Smith N, Tonks S, Voysey M, Mujadidi YF, Mazur O, Rajib NH, Hossen MI, Ahmed SU, Khan A, Rahman N, Babu G, Greenland M, Kelly S, Ireen M, Islam K, O'Reilly P, Scherrer KS, Pitzer VE, Neuzil KM, Zaman K, Pollard AJ, Clemens JD, Protection by vaccination of children against typhoid fever with a Vi-tetanus toxoid conjugate vaccine in urban Bangladesh: A cluster-randomised trial. Lancet 398, 675–684 (2021). [PubMed: 34384540]
51. Waddington CS, Darton TC, Jones C, Haworth K, Peters A, John T, Thompson BA, Kerridge SA, Kingsley RA, Zhou L, Holt KE, Yu L-M, Lockhart S, Farrar JJ, Sztein MB, Dougan G, Angus B, Levine MM, Pollard AJ, An outpatient, ambulant-design, controlled human infection model using escalating doses of Salmonella Typhi challenge delivered in sodium bicarbonate solution. Clin. Infect. Dis 58, 1230–1240 (2014). [PubMed: 24519873]
52. Tan YC, Kongpachith S, Blum LK, Ju CH, Lahey LJ, Lu DR, Cai X, Wagner CA, Lindstrom TM, Sokolove J, Robinson WH, Barcode-enabled sequencing of plasmablast antibody repertoires in rheumatoid arthritis. Arthritis Rheumatol. 66, 2706–2715 (2014). [PubMed: 24965753]
53. Volpe JM, Cowell LG, Kepler TB, SoDA: Implementation of a 3D alignment algorithm for inference of antigen receptor recombinations. Bioinformatics 22, 438–444 (2006). [PubMed: 16357034]
54. Ackerman ME, Moldt B, Wyatt RT, Dugast AS, McAndrew E, Tsoukas S, Jost S, Berger CT, Sciaranghella G, Liu Q, Irvine DJ, Burton DR, Alter G, A robust, high-throughput assay to determine the phagocytic activity of clinical antibody samples. J. Immunol. Methods 366, 8–19 (2011). [PubMed: 21192942]
55. Fischinger S, Fallon JK, Michell AR, Broge T, Suscovich TJ, Streeck H, Alter G, A high-throughput, bead-based, antigen-specific assay to assess the ability of antibodies to induce complement activation. J. Immunol. Methods 473, 112630 (2019).
56. Pearson WR, An introduction to sequence similarity ("homology") searching. Curr. Protoc. Bioinformatics 42, 3.1.1–3.1.8 (2013).

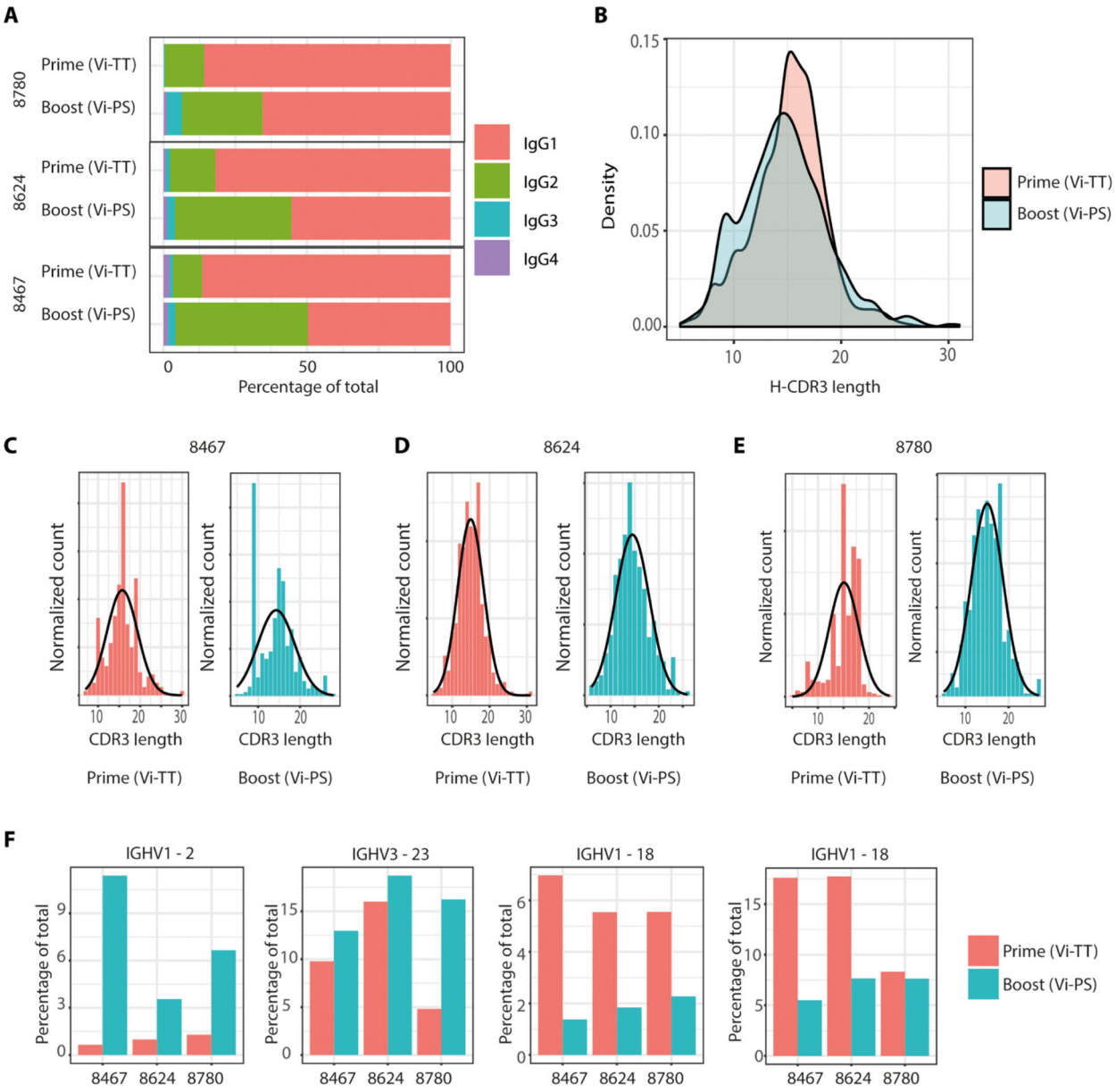

Fig. 1. Sequence characteristics of BCRs from IgG-positive plasmablasts isolated after Vi-TT primary or Vi-PS boost immunization.

(**A**) Subclass distribution for $n = 3$ participants, in response to prime (Vi-TT) and boost (Vi-PS) in a paired fashion. (**B**) Heavy-chain CDR3 length after Vi-TT prime ($n = 3$) or Vi-PS-boost ($n = 3$), showing paired samples only. (**C** to **E**) Individual heavy-chain CDR3 length after Vi-TT prime or Vi-PS boost. Gray lines are based on a normal distribution with the mean and SD of the CDR3 length data for sample shown. (**F**) Ig heavy-chain variable region usage in paired samples, comparing Vi-TT prime and Vi-PS boost. Four heavy-chain regions of interest are shown. Further regions are shown in fig. S4.

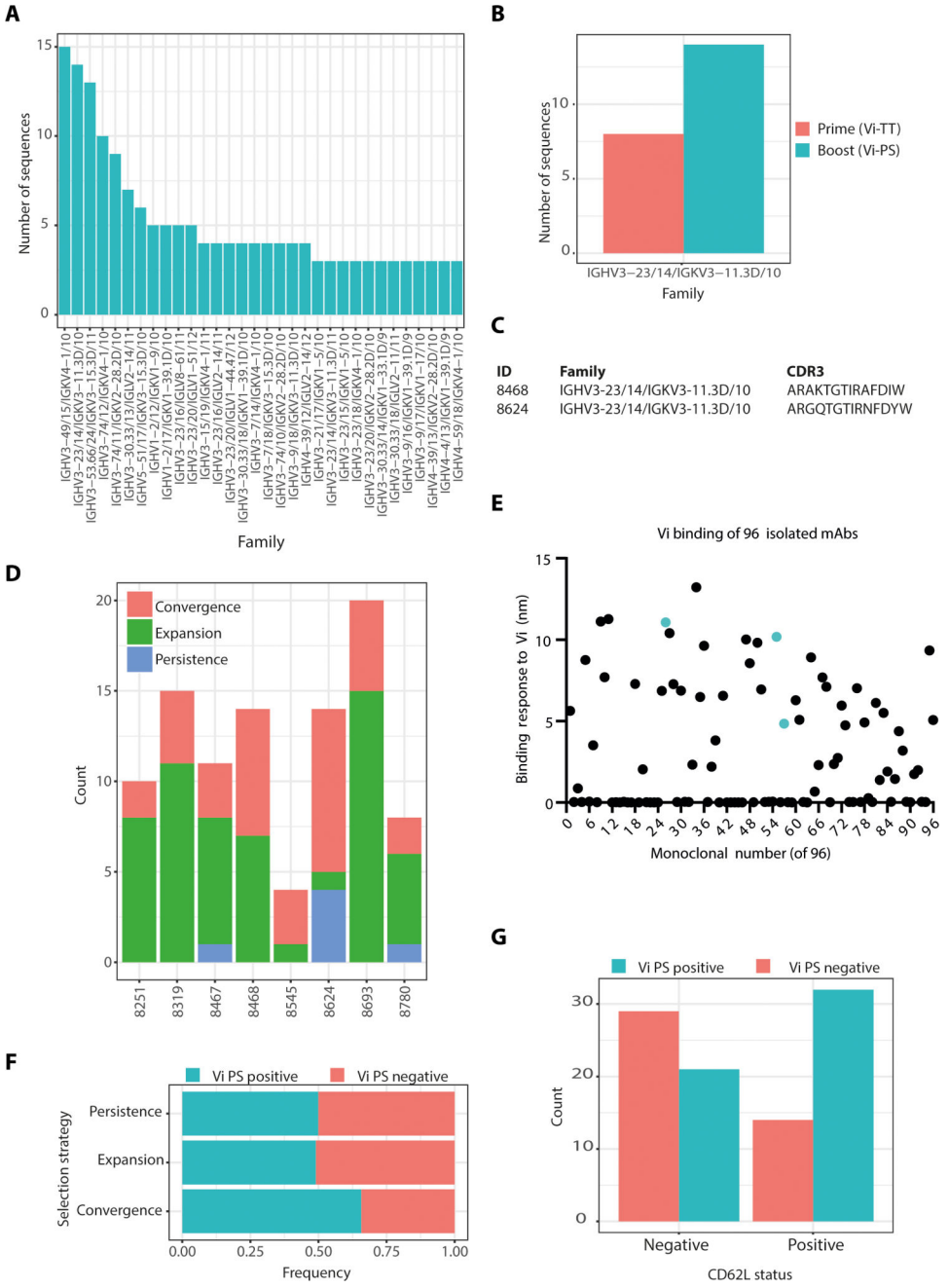

Fig. 2. Selection strategy for the identification of Vi-specific mAbs.

(**A**) Family size of sequences identified in participant 8624 after Vi-PS boost. Families with fewer than three sequences were excluded for the purpose of visualization. (**B**) Example of a family from 8624, selected on the basis of a combination of expansion and persistence. (**C**) Example of a selected convergent antibody pair. (**D**) Strategy used to select each of the 96 mAbs, split by each of the different donors. Antibodies categorized on the basis of persistence were also expanded. (**E**) Vi binding of $n = 96$ isolated mAbs by BLI, where blue dots indicate mAbs isolated from prime time point. (**F**) Frequency of Vi binding mAbs

for each of the selection strategies used, as measured by BLI. (**G**) Vi status of the $n = 96$ selected monoclonals, stratified by CD62L status.

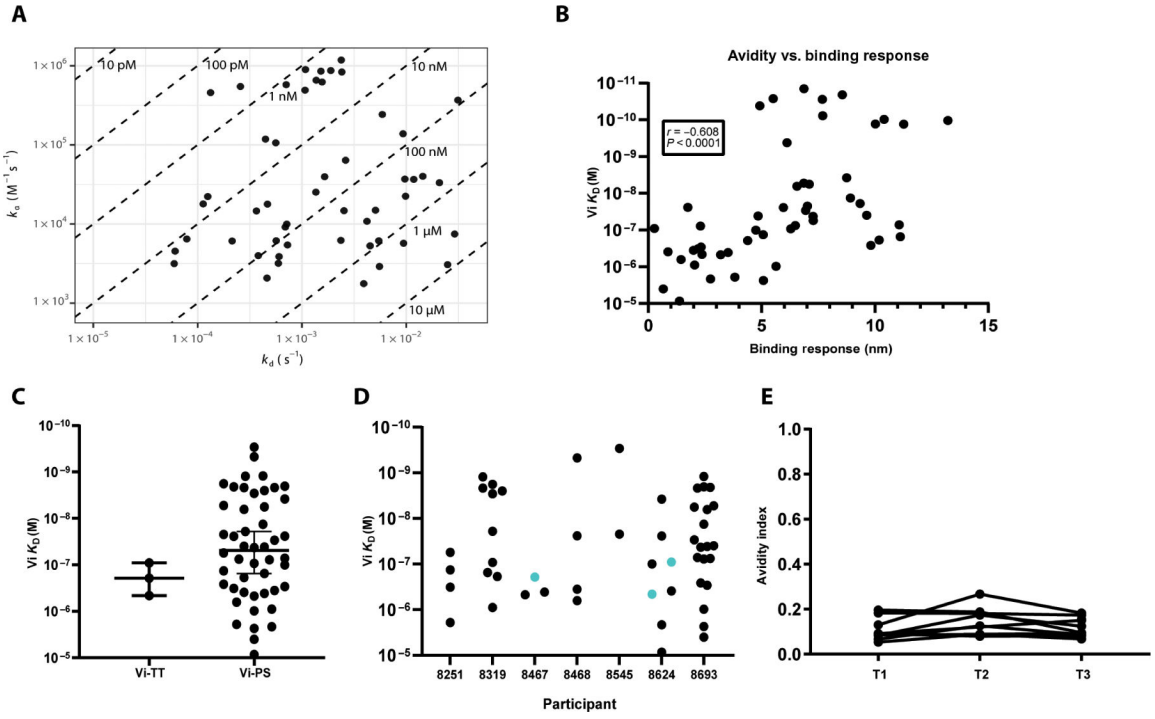

Fig. 3. No evidence for affinity maturation of Vi polysaccharide antibodies after repeat vaccination.

(**A**) Isoaffinity plot indicating avidity measurements for mAbs ($n = 53$) to polymeric Vi polysaccharide by BLI. Diagonal lines indicate the K_D values shown. (**B**) Spearman correlation of Vi antibody avidity and binding response to Vi antigen. Negative correlation represents decrease in K_D, which corresponds to an increase in avidity. (**C**) Avidity measurements (K_D) of Vi binding mAbs stratified by Vi-TT prime/Vi-PS boost. (**D**) Avidity measurements (K_D) of Vi binding mAbs stratified by participant, with blue indicating mAbs from prime time points. (**E**) Total serum (T1, $n = 10$; T2, $n = 8$; T3, $n = 10$) was used to measure residual Vi antibody binding after NaSCN exposure for 15 min in ELISA, as a proxy for avidity measurements. The avidity index was calculated as absorbance at 1 M NaSCN/(absorbance at 0 M NaSCN − absorbance at 5 M NaSCN). T1, 28 days after prime; T2, before Vi-PS boost; T3, 28 days after Vi-PS boost.

A

	Participant ID, time point	mAb	IGHV	V_H CDR3	IGLV	V_L CDR3	Avidity (K_D) M
G1	8624, -21 8467, -21	7977 7994	3-23	ARGRVATIRDFDYW ARGRVATIRDFDYW	3-11κ	QQRNNWPLTF QQRSNWPLTF	1.93E−07 4.59E−07
G2	8693, V2 8545, V2	7972 7981	3-23	AKSPVRGLIRDWYFDLW AKSPARGTNRYWYFDLW	3-20κ	QQYGSSPWTF QQYGSSPYTF	3.56E−07 2.92E−10
G3	8624, V2 8624, V2 8251, V2 8251, V2	7968 7992 7993 8026	3-23	AKGATGTIRAFDYW ARGQTGTIRNFDYW AKGHTGTIRDFDYW AKGATATIRAFDYW	3-11κ	QQRSNWPITF QQRSNWPITF QQRSNWPLTF QQRSNWPITF	1.34E−07 2.43E−08 2.14E−06 3.22E−07
G4	8693, V2 8319, V2	7983 8000	3-74	ARGSSAAAGTYYWFDPW ARGRSAMAGTFYWFDPW	3-15κ	QQYNKWPQTF QQYNKWPQTF	2.17E−09 1.34E−08
G5	8624, V2 8467, V2	7976 7991	2-5	AHRRGTGWYRGVDYW AHRRGTGWYVGLDYW	2-28κ	MQALQTPCTF MQALQTPGSF	4.70E−07 1.00E−07

Amino acid similarity: ○ **Identical amino acids** ○ Similar amino acids (similar chemical characteristics) ○ Different amino acids

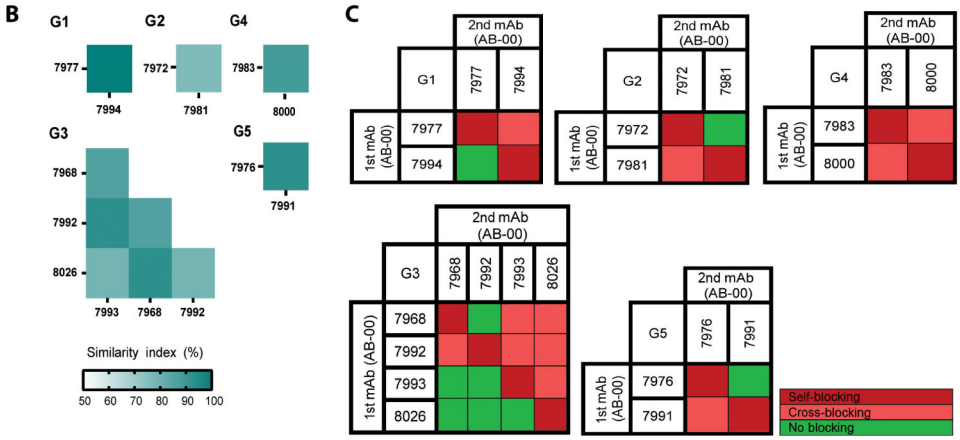

Fig. 4. Convergent development of Vi-specific antibody sequences among Vi vaccine recipients.

(**A**) mAbs (n = 12) from vaccinees with the same variable heavy-chain gene segment were grouped and tested for similarity on the amino acid level by calculating the Levenshtein edit distance. Sequences from vaccinees with ≥75% identity were defined as a convergent group (G1 to G5). Convergent groups based on variable heavy- and light-chain gene segment usage with participant, time point, H- and L-CDR3 sequence, and antibody avidity for Vi antigen. Bold black letters indicate identical amino acids, teal letters indicate amino acids with similar chemical characteristics, and pink letters indicate different amino acids. Chemical characteristics were defined by grouping amino acids based on electrically charged, polar uncharged, and hydrophobicity. (**B**) Quantification of H-CDR3 sequence similarity by BLOSUM62 calculation of similarity index. (**C**) Cross-competition of convergent antibodies within convergent groups by BLI, where the first mAb was bound to Vi to complete saturation before association with the second mAb. Red indicates self-blocking, pink indicates cross-blocking, and green indicates no blocking.

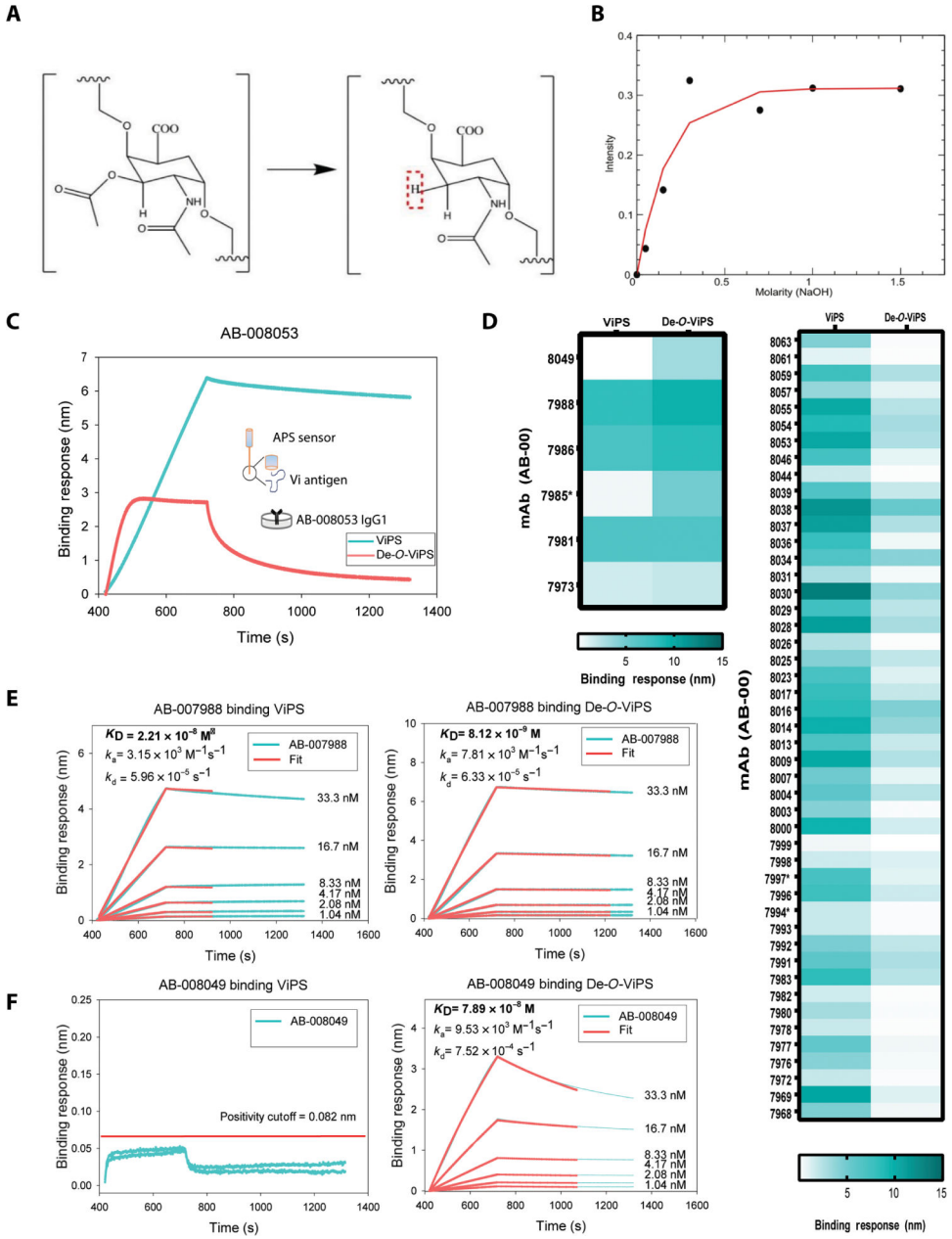

Fig. 5. Antibodies derived from Vi vaccinees recognize de–*O*-acetylated Vi.

(**A**) Molecular structure of Vi polysaccharide monomer with C3 *O*-acetyl conversion to ^{1}H after NH_4OH treatment. (**B**) Increasing signal intensity of two-dimensional NMR spectra centered around 1.9 ppm (^{1}H) and 26.5 ppm (^{13}C), where new C3 ^{1}H-^{13}C bond appears as a function of increasing amounts of NH_4OH treatment ($n = 7$) of polysaccharide for de–*O*-acetylation. (**C**) Binding sensorgram of AB-008053 IgG1 to Vi PS and De-*O*-Vi PS, where Vi is immobilized on biosensor and dipped into wells containing antibody. (**D**) Heatmap of binding response of all Vi binding mAbs ($n = 53$) to Vi PS and De-*O*-Vi PS antigens. Asterisk indicates that mAb was selected after Vi-TT prime. Left: mAbs with equal or greater binding to De-*O*-Vi PS compared with Vi PS ($n = 6$). Right: mAbs with

diminished binding to De-*O*-Vi PS compared with Vi PS ($n = 47$). (**E** and **F**) Example binding sensorgrams of mAbs interacting similarly (E) to Vi PS (left) and De-*O*-Vi PS (right) or better (F) to De-*O*-Vi PS with corresponding avidity measurements indicated. Φ indicates lower antigen density used for antibody titration to reliably measure rate constants.

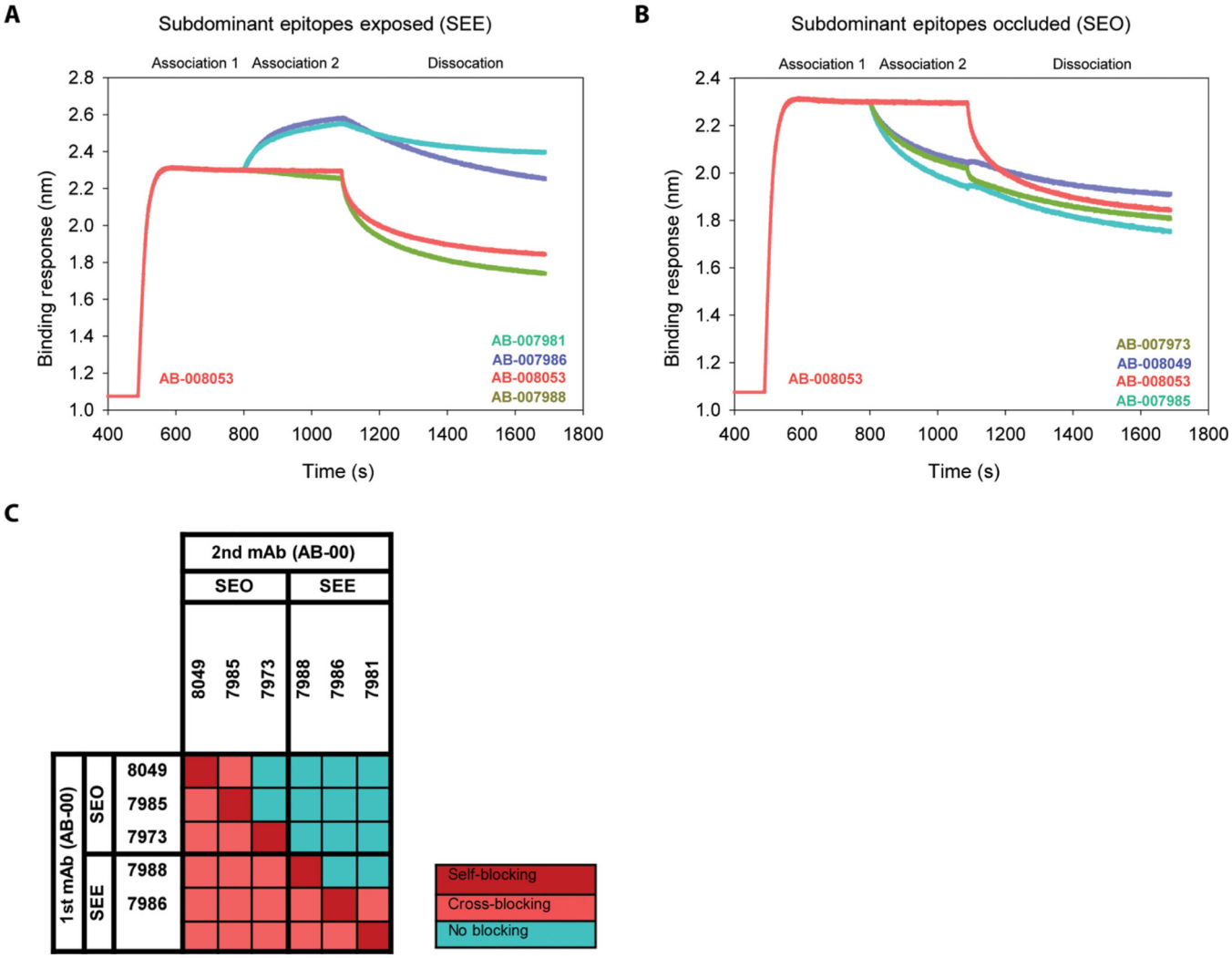

Fig. 6. Vi PS mAbs recognize exposed and occluded epitopes.

(**A**) Competition sensorgram of *O*-acetyl targeting mAb AB-008053 as antibody 1 followed by antibodies ($n = 3$) targeting a subdominant but exposed epitope (SEE) as antibody 2. (**B**) Competition sensorgram of *O*-acetyl targeting mAb AB-008053 as antibody 1 followed by antibodies ($n = 3$) targeting a subdominant and occluded epitope (SEO) as antibody 2. (**C**) Cross-competition matrix of SEE ($n = 3$) and SEO ($n = 3$) targeting mAbs against each other with colored gradient, with blue indicating no blocking and pink indicating cross-blocking.

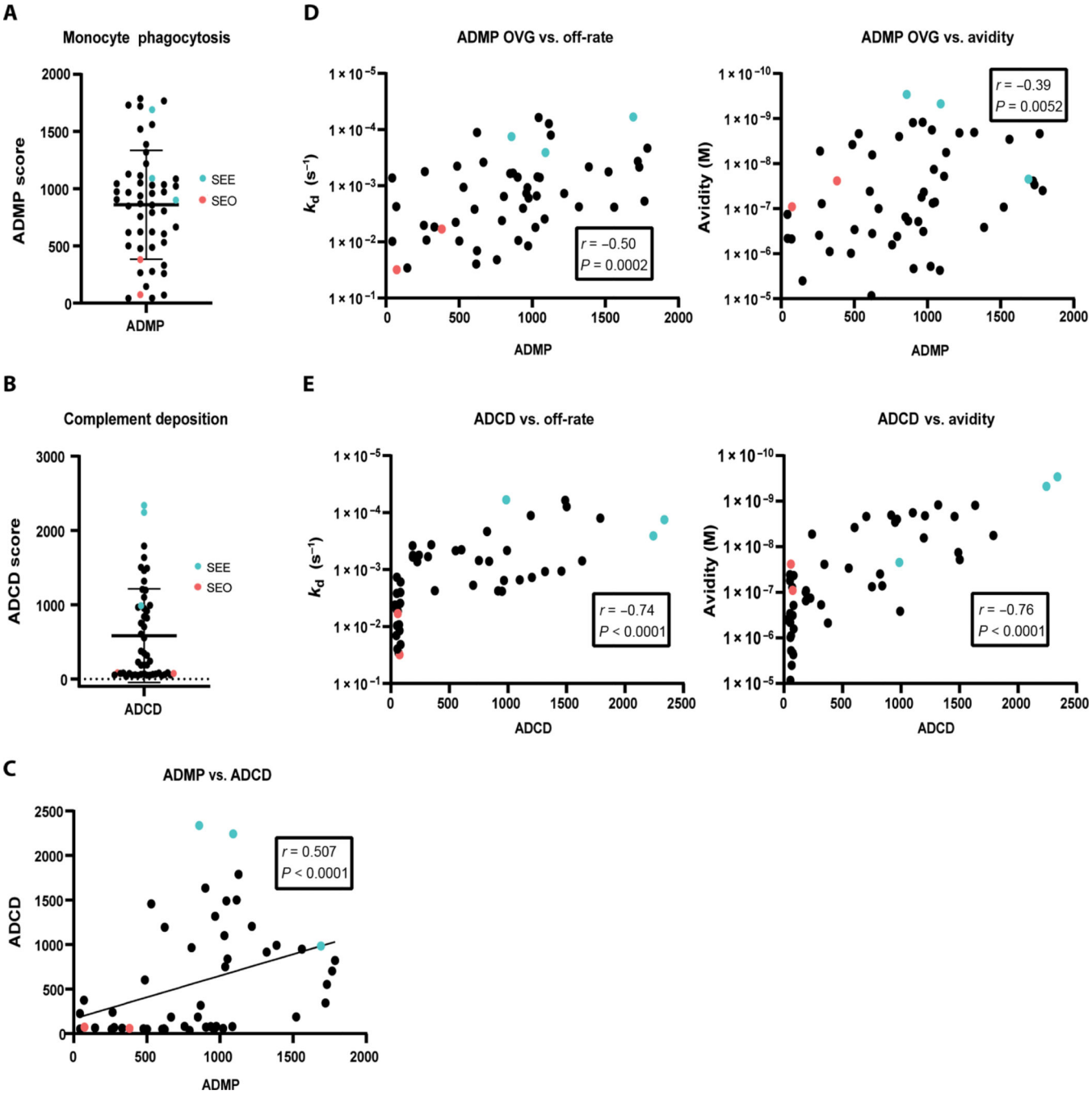

Fig. 7. Vi PS antibodies mediate non-neutralizing Fc effector functions that are highly associated with slow antibody dissociation rates.

(**A**) ADMP scores and (**B**) ADCD scores for Vi binding mAbs ($n = 53$), where blue indicates antibodies that bind to subdominant exposed epitopes (SEE, $n = 3$) and pink indicates antibodies that bind to subdominant occluded epitopes (SEO, $n = 3$). (**C**) Spearman correlation of ADMP and ADCD scores for Vi mAbs ($n = 53$). (**D**) Spearman correlations of ADMP with antibody off-rate (left) and avidity (right). (**E**) Spearman correlations of ADCD

with antibody off-rate (left) and affinity (right). Negative correlations represent decreases in off-rate and K_D, which corresponds to increases in avidity.